ACCOUNTS of chemical research

Article

pubs.acs.org/accounts

Microgel Mechanics in Biomaterial Design

Shalini Saxena,[†,‡,∥] Caroline E. Hansen,[‡,§,∥] and L. Andrew Lyon*[,‡,§]

[†]School of Materials Science and Engineering, [‡]Petit Institute for Bioengineering and Bioscience, and [§]School of Chemistry and Biochemistry, Georgia Institute of Technology, Atlanta, Georgia 30332, United States

CONSPECTUS: The field of polymeric biomaterials has received much attention in recent years due to its potential for enhancing the biocompatibility of systems and devices applied to drug delivery and tissue engineering. Such applications continually push the definition of biocompatibility from relatively straightforward issues such as cytotoxicity to significantly more complex processes such as reducing foreign body responses or even promoting/recapitulating natural body functions. Hydrogels and their colloidal analogues, microgels, have been and continue to be heavily investigated as viable materials for biological applications because they offer numerous, facile avenues in tailoring chemical and physical properties to approach biologically harmonious integration. Mechanical properties in particular are recently coming into focus as an important manner in which biological responses can be altered.

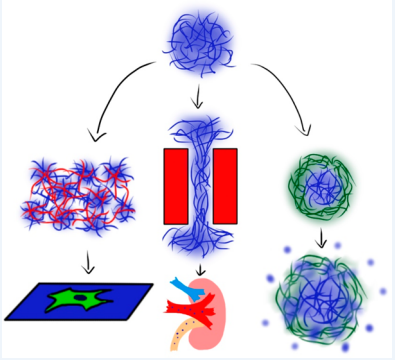

In this Account, we trace how mechanical properties of microgels have moved into the spotlight of research efforts with the realization of their potential impact in biologically integrative systems. We discuss early experiments in our lab and in others focused on synthetic modulation of particle structure at a rudimentary level for fundamental drug delivery studies. These experiments elucidated that microgel mechanics are a consequence of polymer network distribution, which can be controlled by chemical composition or particle architecture. The degree of deformability designed into the microgel allows for a defined response to an imposed external force. We have studied deformation in packed colloidal phases and in translocation events through confined pores; in all circumstances, microgels exhibit impressive deformability in response to their environmental constraints.

Microgels further translate their mechanical properties when assembled in films to the properties of the bulk material. In particular, microgel films have been a large focus in our lab as building blocks for self-healing materials. We have shown that their ability to heal after damage arises from polymer mobility during hydration. Furthermore, we have shown film mobility dictates cell adhesion and spreading in a manner that is fundamentally different from previous work on mechanotransduction. In total, we hope that this Account presents a broad introduction to microgel research that intersects polymer chemistry, physics, and regenerative medicine. We expect that research intersection will continue to expand as we fill the knowledge gaps associated with soft materials in biological milieu.

1. INTRODUCTION

The field of biomaterials has grown concurrently with advances in polymer chemistry, applying new technology to biological applications such as drug delivery, wound healing, and tissue scaffolds.[1] Biocompatibility is an obvious yet challenging hurdle for any biomaterial, where the material must not only be nontoxic and avoid foreign body reactions but, depending on the specific application, might also need to be nonfouling and promote cell infiltration, proliferation, and/or differentiation.[2,3] An ideal biomaterial might be expected to promote regenerative biological pathways for reconstructive healing and degrade over a time scale coinciding with tissue regeneration.[3] Honing biologically integrative properties such as amphiphilicity, functional group identity/density, charge density, size, shape, and biodegradability offers routes to enhance the biocompatibility of polymeric materials.[4−8] However, only recently have researchers tailored mechanical properties to mimic the target system's mechanics as a method to enhance a material's integration into a mammalian host.[9] By mimicking elasticity ranges of biological tissues (∼0.5 kPa for soft tissue (e.g., brain), ∼10 kPa for moderate tissue (e.g., muscle), and >30 kPa for hard tissue (e.g., bone)) in a biomaterial, one can influence cellular response to that material, which can then prolong circulation times for drug delivery vehicles or facilitate cell proliferation on tissue scaffolds.[9,10] Importantly, substrate stiffness has been shown to influence cellular adhesion, cytoskeletal formation, and the differentiation of stem cells.[11,10]

Historically, hydrogels have represented an intriguing class of materials for biological interfacing. Hydrogels are hydrated polymer networks, with mechanical properties somewhat matched to natural tissues, which can enhance biological interactions and improve integration.[12−14] For example, Merkel et al. used their PRINT technique to fabricate red blood cell mimics composed of poly(2-hydroxyethyl acrylate-*co*-poly(ethylene glycol) diacrylate) hydrogels (∼6 μm in ellipsoid size).[15] The investigators monitored in vivo circulation times of the particles in mice as a function of elasticity. Cross-linker concentration was used to modulate particle bulk modulus to achieve values ranging from 63.9 ± 15.7 to 7.8 ± 1.0 kPa. It was

Received: March 26, 2014
Published: May 29, 2014

   dx.doi.org/10.1021/ar500131v | *Acc. Chem. Res.* 2014, 47, 2426−2434

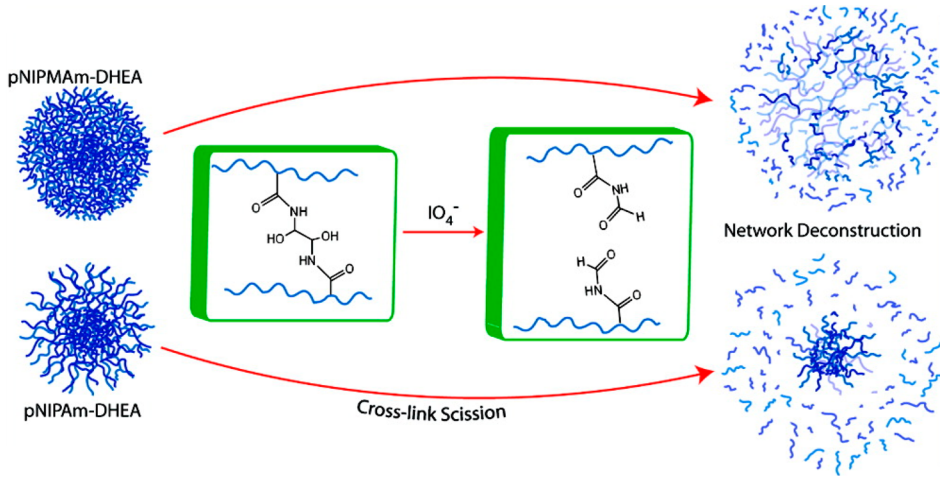

Figure 1. (Top) Erosion of pNIPMAm-DHEA microgels and (bottom) erosion of pNIPAm-DHEA microgels. Adapted with permission from ref 22. Copyright 2011 American Chemical Society.

clearly shown that particle circulation times increased with decreasing modulus, enabling passage through (and therefore limiting deposition in) the lungs and kidneys for particles with the lowest modulus.

While macroscopic hydrogels are appropriate for some biological applications, there are numerous applications wherein nano- to micrometer length scales are important.[16,17] Microgels are similar to hydrogels in that they comprise a solvent swollen polymer network. However, microgels are colloidal particles with dimensions ranging from tens of nanometers to many micrometers, enabling their interfacing with cellular and subcellular domains.[4] Characteristics such as porosity, charge, segment density, amphiphilicity, size, degradability, and softness can be tuned by selecting specific synthetic conditions, monomers, and monomer ratios. For 2D and 3D assemblies of microgels, the softness of the matrix can further be adjusted through covalent or noncovalent intermicrogel cross-linking.[16] For example, Jia et al. used a hyaluronic acid for in situ construction of a microgel network to repair damaged canine vocal folds.[16] The investigators compared the viscoelastic range of microgel networks with and without covalent intermicrogel cross-linking to the viscoelasticity of undamaged canine vocal chords. Full recovery of the entire viscoelastic range (and presumably the ultimate function) was only achieved in the network containing a significant level of intermicrogel cross-linking.

Not only do external cross-links provide an additional handle to modify biomaterial mechanics, they allow for microgel solutions to be physically gelled in situ after injection to the target site. Such an option is attractive from a logistical perspective because it is less invasive than the surgical implantation typically required for macroscopic hydrogel scaffolds.[16,18] Saunders et al. utilized the in situ gelling methodology to introduce load bearing scaffolds into damaged intervertebral discs (IVDs) as an alternative to traditional, high-risk spinal implantation surgery for IVD repair.[18,19] A solution of poly(methyl methacrylate-*co*-methacrylic acid-*co*-ethylene glycol dimethacrylate) microgels functionalized with glycidyl methacrylate was injected into the tissue free space of damaged bovine IVDs. A pH-triggered fluid-to-gel transition was utilized to gel the microgel solution in vitro while covalent intermicrogel cross-links were formed via free radical chemistry. The investigators showed that the microgel network restored mechanical properties of IVDs to ranges observed in undamaged IVDs and showed little cytotoxicity toward human nucleus pulposus cells, making the doubly cross-linked microgel approach viable for IVD repair.

The rising importance of mechanics in practical biomaterials has spurred a heavy investigation of microgel mechanics, revealing highly tunable mechanical properties at all scales. In this Account, we focus on the emerging importance of microgel mechanical properties in our work. More specifically, we discuss how microgel mechanics have inadvertently emerged as critical parameters through fundamental investigations of microgels as colloidal building blocks and delivery vehicles. Upon realization of the dynamic mechanical possibilities microgels possess, we have investigated the purposeful tuning of macroscopic microgel assemblies to achieve specific biological outcomes.

2. DESIGNING MICROGELS

Fundamental studies of microgels originally focused on understanding the relationship between chemical composition and stimuli (e.g., temperature, pH, ionic strength, and light)[20] triggered swelling and deswelling responses of poly(*N*-isopropylacrylamide) (pNIPAm) or poly(*N*-isopropylmethacrylamide) (pNIPMAm) microgels. While the focus of these experiments was to interrogate microgel behavior, a significant amount of information can be gathered regarding microgel mechanical properties from these early experiments. In particular, we can deduce how chemical composition dictates polymer density and thus controls mechanical behavior at the most rudimentary level.

2.1. Synthetic Control of Polymer Network Density

Adjusting cross-linker concentration is perhaps the most straightforward way to modulate microgel stiffness. Increasing cross-linker content increases polymer (segment) density and subsequently decreases network flexibility. Chain confinement results in an increase in particle density, smaller particle size, and decreased swelling. In addition, reactivity ratios between the monomers and cross-linkers present another path to modulate polymer density. Saunders validated a "core/shell" polymer density structure in pNIPAm microgels cross-linked with either 1% or 10% mol *N*,*N*′-methylenebis(acrylamide) (BIS) using small angle neutron scattering.[21] The cross-linker BIS has a higher reactivity than the monomer NIPAm, resulting

dx.doi.org/10.1021/ar500131v | *Acc. Chem. Res.* 2014, 47, 2426−2434

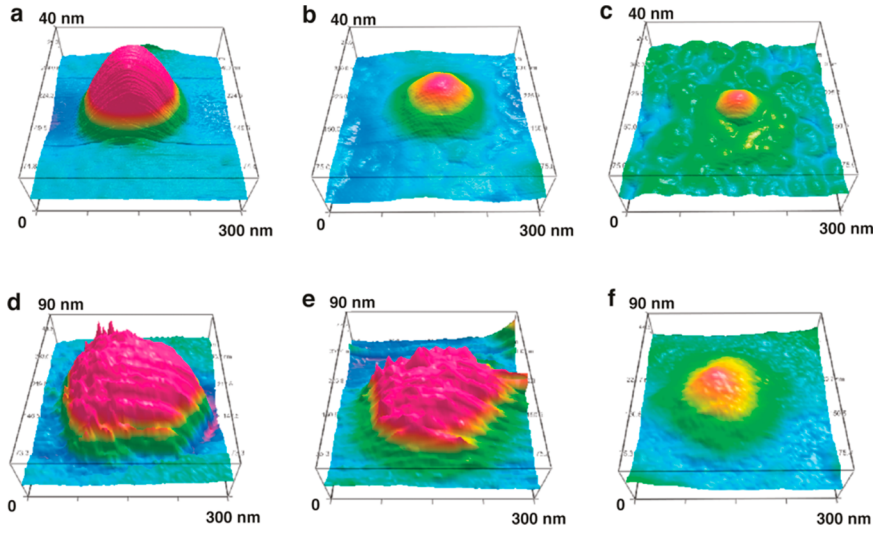

Figure 2. Three-dimensional renderings of AFM images obtained from a single microgel during erosion under deswollen (a–c) or swollen (d–f) conditions at 0 h (a, d), 24 h (b, e), and 434 h (c, f). Reprinted with permission from ref 24. Copyright 2010 American Chemical Society.

in a highly cross-linked core. Because less cross-linker is available toward the end of the reaction, the microgel periphery consists of a low segment density shell with highly flexible polymer chains.

We have also explored how polymer distribution in microgels impacts downstream properties, such as erosion in studies related to the clearance of drug delivery vehicles. Microgels consisting of either pNIPAm or pNIPMAm were synthesized with 10 mol % of degradable cross-linker (1,2-dihydroxyethylene)bis(acrylamide) (DHEA).[22] Microgel degradation was initiated with periodate and monitored via multiangle light scattering (MALS). Degradation of pNIPAm-based microgels produced a nonlinear mass decay beginning at the periphery, with erosion terminating with a remnant particle of branched, presumably core-localized polymer chains (diagram in Figure 1). A chain transfer mechanism is suggested to cause such branching through hydrogen abstraction via either the α-carbon on the amide functionality in the polymer backbone or the tertiary carbon of the isopropyl group, resulting in nondegradable cross-links in the microgels.[23]

In contrast, degradation of pNIPMAm showed a slight increase in size at the onset followed by complete decay of the polymer. Such behavior is indicative of a homogeneous polymer network, where initial cross-link scission affords concomitant network swelling; sizable mass loss occurs only when the network connectivity is decreased enough to liberate soluble chains. The difference in network density between pNIPAm and pNIPMAm is explained by their reactivity ratios with cross-linker. The monomer NIPMAm and cross-linker have similar reactivity ratios resulting in a homogeneous network with higher overall network density. Microgels made from pNIPMAm as a result are noticeably stiffer than pNIPAm microgels, which have a soft periphery of loosely cross-linked chains. Thus, we see that even the selection of the main monomer itself contributes to the large changes in the mechanical properties of individual microgels, their network topology, and pathway of erosion.

In a subsequent investigation, we monitored microgel degradation with atomic force microscopy (AFM) in serum at 37 °C, mimicking a biologically relevant environment. AFM was used to resolve initial particle swelling and mass loss events.[24] PNIPMAm microgels with 2% mol acrylic acid (AAc) were cross-linked with 2% mol *N*,*O*-dimethacryloyl hydroxylamine (DMHA), which is susceptible to base hydrolysis at pH > 5. Microgels were eroded under swollen and collapsed conditions to compare effects of swelling (Figure 2). Under deswollen conditions, a decrease in height by 14% was seen, while microgels imaged under hydrated conditions showed an initial increase in height during erosion. These results corroborate that initial height increase of pNIPMAm is due to swelling caused by initial cross-link scission, even though mass is simultaneously being lost (as shown via imaging under deswollen conditions).

Another important parameter to consider in drug delivery is the ability to load solute within the carrier. For microgels, it is easy to see the correlation between mesh size and loading ability. Protein loading and how it correlates with microgel charge was recently evaluated in our lab using cytochrome *c* (cyt *c*), a positively charged protein.[25] Microgels were composed of pNIPAm, BIS (2% mol), and AAc in varied amounts (10%, 20%, and 30% mol) to impart anionic charges in the microgel, facilitating cyt *c* uptake through Coulombic interactions. MALS revealed the 30% mol AAc microgel loaded significantly more protein per available AAc site than either the 20% or 10% mol acid particles, −0.13 compared to 0.05 and 0.01, respectively.

The drastic increase in loading ability of the 30% mol AAc microgels is attributed to a more porous internal polymer network. The greater amount of internal charge present in the 30% mol AAc microgel leads to a higher internal osmotic pressure. Subsequently, a lower segment density is established during synthesis, allowing more cyt *c* to penetrate further into the microgel. No statistically meaningful difference in binding constants was observed, suggesting that multivalent interactions between AAc and cyt *c* were not a major factor in increased loading. Charged comonomer concentration consequently functions as an important factor for tailoring porosity and subsequent macromolecule loading.

2.2. Control of Mechanics through Exotic Architectures

Early on in our microgel work, we developed methods for the synthesis of well-defined core/shell microgels, which were envisioned to have potential as drug carriers.[26] These microgels

dx.doi.org/10.1021/ar500131v | *Acc. Chem. Res.* 2014, 47, 2426–2434

have different chemical compositions in the core and shell, allowing for multiple characteristics to be employed such as two Volume Phase Transition Temperature's (VPTT) (e.g., ∼31 °C for pNIPAm and ∼45 °C for pNIPMAm) or specific localization of charge and functional groups.[26,27] Core/shell microgels are also of fundamental interest because they exhibit a phenomenon known as core compression, where the shell physically compresses the core.[28]

Core compression occurs because the shell synthesis occurs above the core VPTT. When the solution is cooled to room temperature, the core cannot fully swell due to the presence of the surrounding shell, which essentially acts to "shrink wrap" the core. Furthermore, in constructs where the core monomer has a lower VPTT than the shell monomer, core deswelling cannot fully occur at its native VPTT because shell polymer chains prohibit neighboring core chains from collapsing. Berndt et al. used differential scanning calorimetry (DSC) to study how shell thickness affects core compression and particle collapse thermodynamics.[29] Four pNIPAm core/pNIPMAm shell microgels were studied with varying core/shell mass ratios of 1:0.23, 1:0.69, 1:1.42, and 1:2.50. The DSC of the microgels containing the thickest shell showed three peaks during the phase transition in contrast to the two peaks (corresponding to two clear volume phase transition events) observed for all other shell thicknesses studied (Figure 3). In the thickest shell case, the elastic restoring force of the shell was able to overcome the thermodynamic driving force associated with the phase transition, stretching core chains and creating different hydrogen bonds with the shell polymer chains. The third DSC peak occurred when those new hydrogen bonds were broken and full core collapse was achieved. The balance between the elastic restoring force of the shell and thermodynamic deswelling force of the core is an excellent example of how the mechanical properties of core/shell microgel architectures can be manipulated through spatial synthetic control.

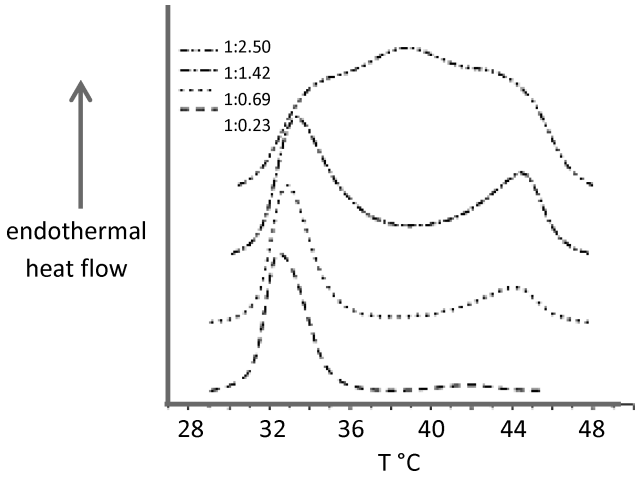

Figure 3. Normalized DSC thermograms of pNIPAm core/pNIPMAm shell microgels with core/shell mass ratios of 1:0.23, 1:0.69, 1:1.42, and 1:2.50 recorded at heating rate of 2 K min^{-1}. Reprinted with permission from ref 29. Copyright 2012 John Wiley and Sons.

We further investigated core/shell structures by means of controlled shell degradation.[30] Microgels consisting of a nondegradable pNIPAm-BIS (2% mol) core and a pNIPMAm shell of varying DMHA cross-linker concentration (2% and 4% mol) were studied. The core/shell particles had roughly the same diameter as the cores alone (measured by MALS), which is an expected result of core compression.[28] Particle deformability was studied with AFM through footprint and height measurements after deposition onto glass. As shown in Figure 4, the cores exhibited a deposited height of 7 ± 1 nm, while core/shell microgels exhibited heights of 32 ± 5 and 30 ± 3 nm for 2% and 4% mol cross-linker concentrations, respectively. The greater particle stiffness seen in the core/shell microgels is attributed to the added connectivity and rigidity imparted by the pNIPMAm shell, as well as the added polymer mass.

Particle diameter after shell degradation was characterized using asymmetrical flow field-flow fractionation coupled to MALS, which resolved an increase in radius of ∼3 and ∼4 nm for both 2% and 4% mol DMHA shells, respectively. Microgel size increases are likely due to core compression alleviation: removal of shell cross-linker and shell density allows the core to approach its full swelling capacity. Spreading of the 2% mol DMHA particle increased by 94 ± 28 nm and height decreased by 20 nm, while the 4% mol DMHA particle's spreading increased by 13 ± 27 nm and height decreased by 8 nm (Figure 5). The observation that 4% mol DMHA microgel changes were smaller than those observed in the 2% mol DMHA case is likely associated with incomplete erosion of the shell in the 4% case. Nonetheless, it is clear deformability and porosity increased as a result of shell degradation for both core/shell constructs, further illustrating how spatial control in core/shell microgels is an effective approach to both chemical and mechanical tuning.

3. MECHANICAL RESPONSE TO ENVIRONMENT

The environment surrounding microgels can have a great influence on their properties through a variety of mechanisms including particle−particle interactions, particle−solvent interactions, external osmotic pressure, temperature, pH, volume fraction, and physical confinement. The deformability of microgels, in contrast to the relative shape invariance of hard spheres, can be seen in classical colloid physics studies investigating phase transitions in monodispersed colloidal dispersions.[31] Previously, we formed colloidal crystal lattices from pNIPAm and BIS (3% mol) microgels (hydrodynamic radius, R_H ∼ 375 ± 20 nm) doped with 0.1 wt % of large "defect microgels" composed of pNIPAm, AAc (10% mol), and BIS (1% mol) (R_H ∼ 873 ± 66 nm). The large microgel "defects" were seamlessly integrated into the bulk lattice without observable structural or dynamic (diffusional) perturbations. The ability for the dopant microgel to fit into the lattice of a 5.5 wt % ($\phi_{eff} \approx 0.66$) sample is impressive, occupying a volume that was roughly 15 times smaller than that of the "defect" dilute solution hydrodynamic diameter. This remarkable ability of microgels to conform to colloidal crystal lattice structures exemplifies the deformability of these materials in response to mechanical and/or osmotic restraints.

When using microgels for biological applications, the influence of mechanics on various cellular and physiological processes must be considered. In discriminatory biological environments in particular, microgel mechanics can be highly influential. Banquy et al. previously investigated the influence of the elasticity of hydrogel nanoparticles on cellular uptake and intracellular fate in murine macrophages.[32] Nanoparticle elasticity was controlled by varying cross-linker concentration

dx.doi.org/10.1021/ar500131v | Acc. Chem. Res. 2014, 47, 2426−2434

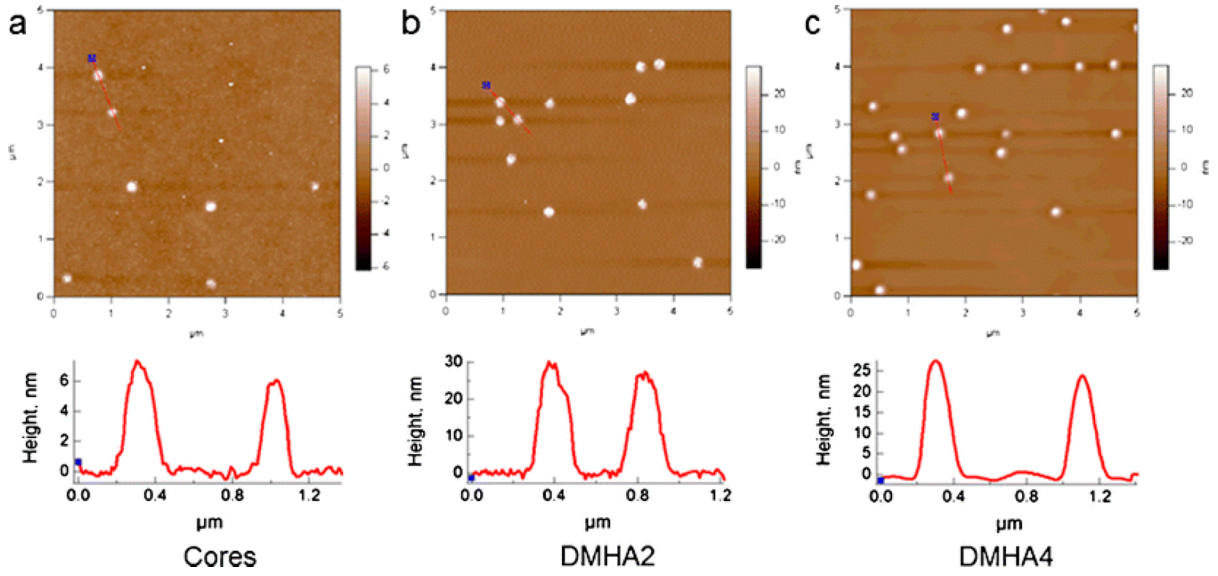

Figure 4. AFM (height) images and height line traces of (a) core particles, (b) 2% mol DMHA core/shell particles, and (c) 4% mol DMHA core/shell particles. Adapted with permission from ref 30. Copyright 2013 Springer.

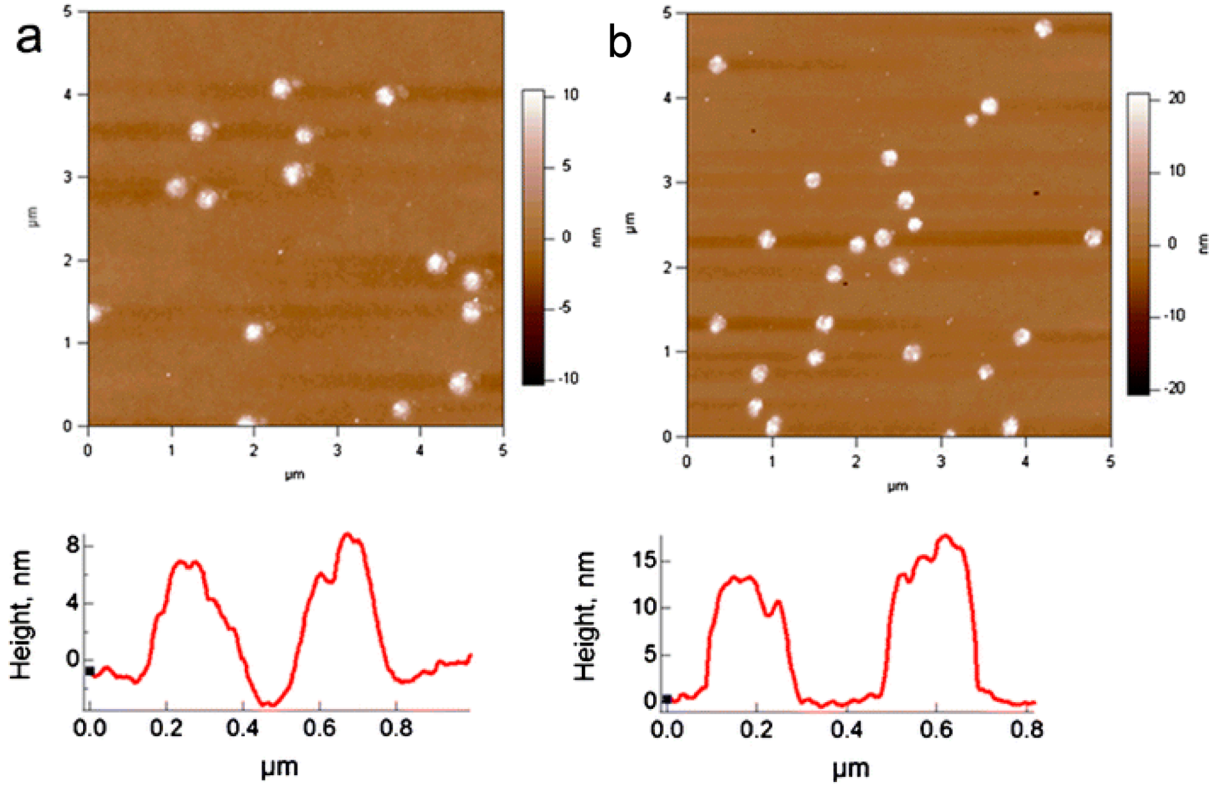

Figure 5. AFM (height) images and height line traces of 2% mol DMHA (a) and 4% mol DMHA (b) following 1 month of erosion in pH 7.4 buffer at 37 °C. Adapted with permission from ref 30. Copyright 2013 Springer.

during emulsion polymerization. Using AFM, the Young's modulus for all nanoparticles was determined; values ranged from 18 ± 4 kPa (1.7% mol cross-linker) to 39 ± 43 kPa (15% mol cross-linker). Investigation of the uptake mechanisms was performed by treating cells with endocytic and metabolic inhibitors prior to incubation with the nanoparticles. The investigators determined that softer nanoparticles, with the lowest Young's modulus (18 ± 4 kPa), were internalized almost exclusively by macropinocytosis. In contrast, more elastic nanoparticles, with slightly higher Young's moduli (35 ± 10 and 136 ± 39 kPa), were internalized via clathrin- and/or caveolae-mediated entry routes. Finally, the stiffest nanoparticles, with the highest Young's modulus (211 ± 43), were internalized mainly by a clathrin-mediated endocytosis. Here we clearly see that when it comes to cellular uptake, the relevant mechanism is highly dependent on nanoparticle softness.

Renal filtration is another biological process that is constrained by a material's mechanical properties, requiring passage of nanoparticles through roughly 8 nm diameter pores

dx.doi.org/10.1021/ar500131v | Acc. Chem. Res. 2014, 47, 2426−2434

under a pressure differential of 40−80 Torr.[33,34] For many rigid nanoparticles, this clearance mechanism provides strict size limitations. In contrast, deformable nanoparticles could potentially overcome these size restrictions, which might result in delivery vehicles that can be eliminated via normal excretion pathways, thereby limiting the amount of nanocarrier hepatic and renal deposition and retention. To investigate this, we have studied microgel deformation by translocation through cylindrical pores under biologically relevant pressure differentials in order to mimic renal filtration.[35]

Track-etch membranes were used to model endothelial pores present in the renal system (Scheme 1). The microgels were composed of pNIPAm, AAc (10% mol), 4-acrylamidofluorescein (0.02% mol), and either 1% mol BIS (R_H ~ 570 nm at pH 7.4) or 3% mol BIS (R_H ~ 433 at pH 7.4). Investigation of translocation of microgels and rigid polystyrene (PS) spheres of similar size indicated that, at pH 7.4, PS spheres exhibited jamming in the pores. In contrast, the deformable microgels did not jam appreciably, and they passed through pores under modest applied pressure. Furthermore, increasing the microgel cross-linker content to 3% mol BIS did not inhibit translocation, even when the pore openings were more than 10-fold smaller than the microgel diameter.

Scheme 1. Filtration Method for Evaluating Microgel Pore Translocation

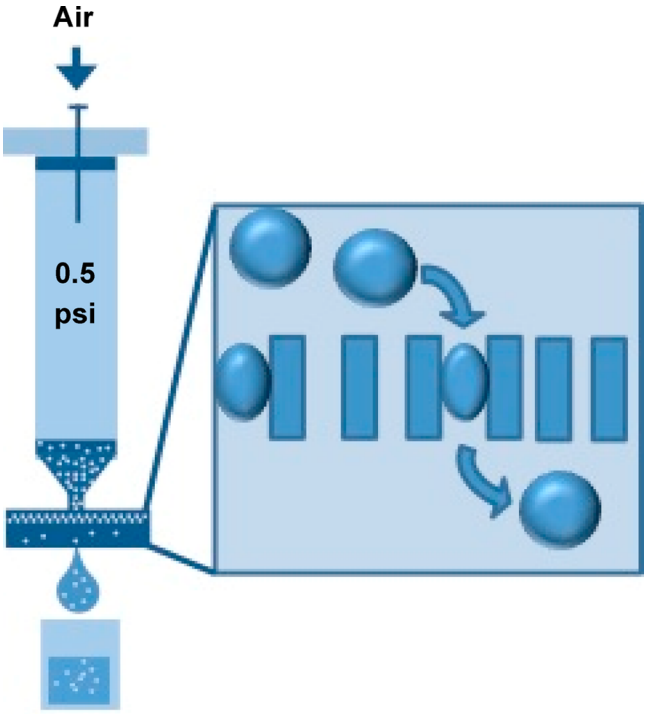

This concept was further investigated using resistive pulse sensing with 25−50 μm thick glass nanopore membranes (GNMs) prepared to contain a single conical pore with orifice radii ranging from 200 to 700 nm.[36] Pressure-driven microgel translocation was monitored, measuring the change in ion current as microgels (dispersed in an electrolyte solution) passed through the pore. Microgels (R_H ~ 570 nm) were composed of pNIPAm, AAc (10% mol), and BIS (1% mol).

When microgels had a diameter smaller than the pore size, a single current peak was observed where the current increased due to the highly charged anionic microgel displacing pore electrolyte during passage. In contrast, when the microgels had a diameter larger than the pore, a more complex peak pattern consisting of multiple current transients was observed. These larger microgels must deform in order to translocate, resulting in an expulsion of electrolyte solution and a subsequent decrease in current from the peak maximum associated with the initial electrolyte displacement. After the microgel passes through the narrowest portion of the pore, the electrolyte solution is reabsorbed, the microgel passes out of the sensing zone, and the current returns to baseline. At higher applied pressures, the single current peak returns, as the two transients seem to collapse into one, suggesting that the microgel deforms and passes through the pore with minimal volume change, indicating the translocation rate is faster than the effective deswelling rate (Figure 6). In these studies, we observed a minimum nanopore-to-microgel radius ratio of ~0.4 for translocation, which suggests a theoretical limit imposed by the compressibility of the microgel and Coulombic repulsion between the microgels and the pore walls. This theoretical limit is largely determined by the properties of the microgel, such as internal density of charged groups, chain flexibility, and strength of the solvent−polymer interactions. These properties can be tuned to adjust microgel mechanics in order to control response to the surrounding (mechanical) environment.

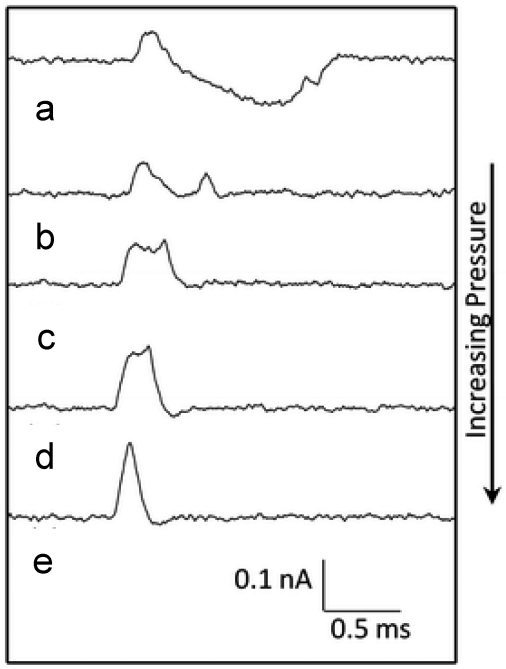

Figure 6. Expanded $i-t$ traces of individual microgel (R_H ~ 570 nm) translocations through a GNM. Traces represent translocation events through a 302 nm radius pore at applied pressures of (a) −70, (b) −80, (c) −100, (d) −120, and (e) −150 mmHg. Reproduced from ref 36 with permission from The Royal Society of Chemistry.

4. MECHANICAL PROPERTIES OF MICROGEL ASSEMBLIES

Moving beyond individual particles, we have interrogated the mechanical properties of self-healing polyelectrolyte multilayer microgel films on multiple scales using a variety of techniques. Recently, our lab investigated microgel film self-healing to gain more insight into the mechanism of film damage and to understand what drives restoration of film integrity.[37] Films

dx.doi.org/10.1021/ar500131v | Acc. Chem. Res. 2014, 47, 2426−2434

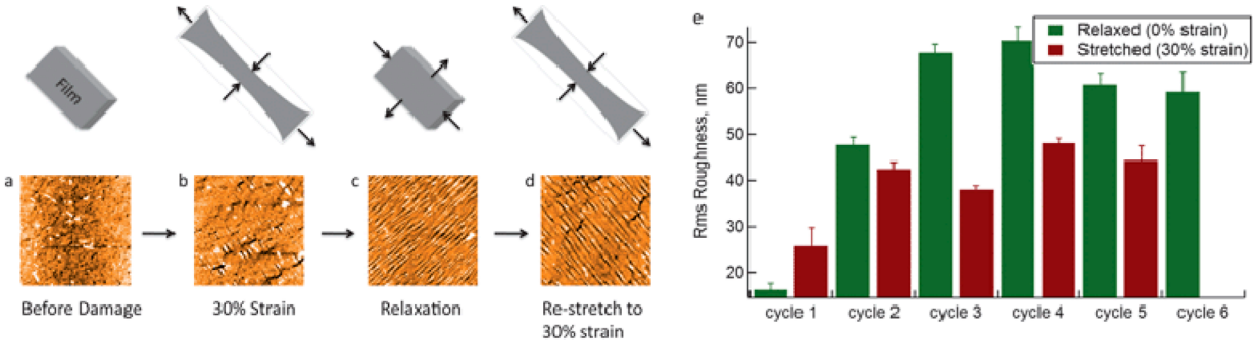

Figure 7. AFM (height) images of microgel multilayer films shown (a) before cycling at 0% strain, (b) at 30% strain, (c) when the film is relaxed back to 0% strain, and finally (d) when the film is restretched to 30% strain. (e) The pattern of roughness persists throughout multiple cycles. All AFM images are 40 μm × 40 μm. Reproduced from ref 37 with permission from The Royal Society of Chemistry.

were assembled using a layer-by-layer (LbL) approach from microgels containing pNIPAm, AAc (10% mol), and BIS (2% mol) and the linear polycation, poly(diallyldimethylammonium chloride) (pDADMAC) on elastomeric poly(dimethylsiloxane) (PDMS) substrates. Dried films were subjected to linear strains between 0% and 30%. We observed that an undamaged film stretched to a strain of 30% then relaxed forms a parallel wrinkled pattern on its surface. However, if the film is then hydrated, the wrinkles disappear and the original film integrity is restored, demonstrating that these films can self-heal.

For an undamaged film that is initially stretched to a strain of 30% and is then relaxed (Figure 7a–c), the resulting wrinkles lie orthogonal to the stretching axis, which suggests a buckling behavior following plastic deformation of the microgel film. If the same film is restretched to 30% strain in the same direction (Figure 7d), the wrinkles appear to reorient themselves orthogonal to the original pattern (parallel to the direction of strain). This directional change results from elongation and compression forces experienced by the film during stretching on the elastomeric PDMS substrate. During the initial stretching period, the PDMS substrate elongates along the stretching axis and compresses along the perpendicular axis. If we assume the entire film must also undergo some degree of deformation during the initial stretching event, the in-plane film axis perpendicular to the initial stretching axis is under compression during a second stretching event. This compression creates a new wrinkling pattern perpendicular to the stretching axis. Upon relaxation of the stress, the effective surface area of the substrate is reduced, inducing wrinkling of the film that occurs because of the elasticity mismatch between the film and the underlying PDMS substrate.

Because individual microgels are connected via noncovalent (Coulombic) interactions between pDADMAC and AAc sites, these weak bonds can be sacrificed in favor of an altered ion pairing structure. This allows for an increase in film dimension along the stretching axis to dissipate the stress and prevent failure. Because there is a mismatch in elasticity between the multilayer and the PDMS substrate, the disrupted interactions cannot recover at the same rate as the PDMS, resulting in wrinkling of the elongated film. During hydration, the polymer and ion mobility that occurs allows restoration of the smooth, low-energy confirmation.

In this complex structure, polymer chain flexibility and particle deformability allow for self-healing to occur under hydrating conditions. Such softness has given microgel films an additional application in the area of nonadhereing coatings. Building upon an investigation by Yamato et al. to harvest keratinocytes on culture dishes grafted with pNIPAm,[38] Schmidt et al. demonstrated the ability to use pNIPAm-BIS (6 mol % cross-linker) microgel films cross-linked with poly(ethylenimine) (PEI) for thermally controlled detachment of adsorbed fibroblasts.[39] After a 48 h incubation at 37 °C in cell culture medium, fibroblasts were observed to adhere and spread well. After cooling to 20 °C, the cells exhibited a round morphology (effectively detached) and were removed from the surface with gentle washing. Successive cycles of spreading/rounding were also observed, indicating a reversible behavior. Cell detachment from microgel coatings may be attributed to increased hydration of the polymer, reducing attractive van der Waals interactions and increasing repulsive osmotic interactions. Ellipsometry and AFM measurements indicated that upon crossing the VPTT the water content changed from 90 wt % to less than 30 wt % and the elastic modulus of the microgels increased by an order of magnitude. At 37 °C, the water content was 70 wt % and the modulus was in the range of several hundred kilopascals, making the substrate more suitable for cell adhesion.

In contrast to the use of hydrophilic/hydrophobic interactions to influence cell adhesion, we investigated the influence of the unique mechanical properties of self-healing microgel films on fibroblast adhesion.[40] We fabricated polyelectrolyte films with anionic microgels composed of pNIPAm and AAc (30 mol %), with either BIS or poly(ethylene glycol) diacrylate (PEGDA) (4 mol %) as the cross-linker. Either pDADMAC or PEI was used as the polycation for film construction. All films showed high protein adsorption, yet multilayers showed low fibroblast adhesion in comparison to monolayers. This finding indicates the presence of a nonadherent mechanism that is independent of a nonfouling behavior, which could be due to the unique properties associated with film mobility and self-healing. To test this, the films were chemically cross-linked to reduce polymer mobility and the influence of film mobility was evaluated in the context of cell adhesion and spreading. pDADMAC films served as negative controls for the cross-linking process because pDADMAC lacks the primary amines required for cross-linking via EDC/NHS coupling.

AFM nanoindentation data indicated that all films were "physiologically stiff," having Young's moduli greater than 30 kPa.[10] The cross-linked BIS/PEI films exhibited the highest Young's modulus, approximately an order of magnitude higher than that of the uncross-linked BIS/PEI film. All films absorbed large amounts of protein regardless of microgel composition or cross-link treatment. As shown in Figure 8, fibroblast adhesion was minimal in uncross-linked multilayers and any observed

dx.doi.org/10.1021/ar500131v | Acc. Chem. Res. 2014, 47, 2426–2434

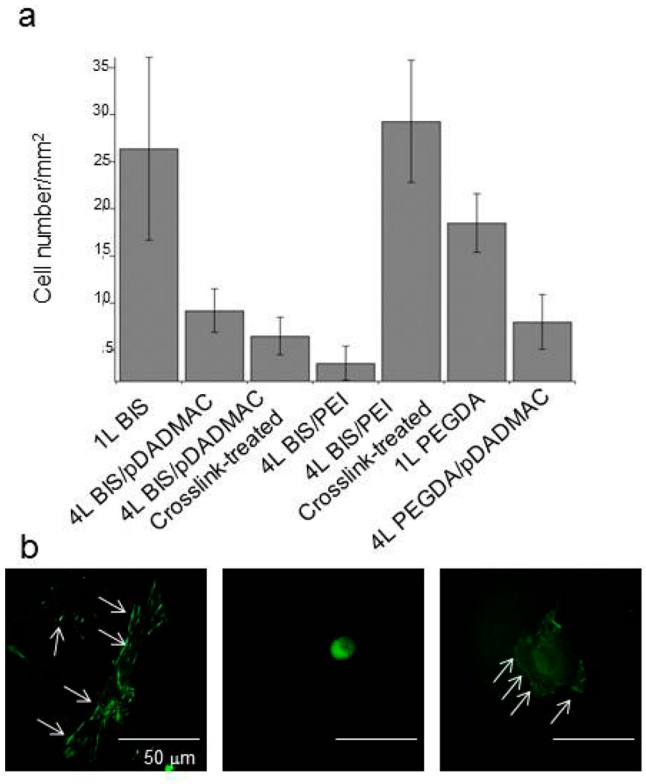

Figure 8. (a) Fibroblast numbers on various films indicated a higher cell count on monolayers and the BIS/PEI cross-linked films and a lower count on untreated multilayers. (b) Vinculin staining of fibroblasts cultured on monolayer BIS (left), multilayer uncross-linked BIS/PEI (middle), and multilayer cross-link treated BIS/PEI (right) films illustrates the relative maturity and presence of focal adhesions on the different films. Reproduced from ref 40 with permission from The Royal Society of Chemistry.

cells were poorly spread. However, fibroblasts exhibited a spread morphology on the cross-linked BIS/PEI films and monolayer films with high degrees of cell attachment. At the microscale, these results can potentially be attributed to the polymer mobility within the films, where microgel and polyelectrolyte mobility decreases with increasing intermicrogel cross-linking. At the nanoscale, this behavior can be attributed to the viscoelastic character of the microgels and the intervening polycation in the film. Fibroblasts cannot form focal adhesions to uncross-linked films because microgels shift underneath the fibroblast as they feel the force of the fibroblast probing the surface, resulting in nonadherent material properties. In this fashion, we are able to observe the importance of microgel film mechanics on multiple length scales at the cell–substrate interface.

5. CONCLUSIONS AND OUTLOOK

The importance of microgel mechanical properties in the literature has progressed with the realization of their impact in biological environments. Microgels offer a bottom-up and multiscale route by which mechanics can be tailored on the individual level from particle synthesis or in assemblies through intermicrogel cross-links. Specific ranges of modulus control can be achieved providing control over material response to its environment and cellular responses to the material. The ease of synthesizing microgels to display a wide range of mechanical properties on the particle level and in assemblies affords microgel-based materials real potential in a variety of biomedical applications. We have envisioned a new set of microgel-based materials for the next generation of regenerative medicine, wound healing, and other biomedical tools, as a new frontier for microgel-related research. Currently, our group has ongoing investigations in the development of peptide-modified microgels for applications in hemostasis, microgel/fibrin composites matrices to control/direct cell phenotype, self-assembled peptide/microgel composites for use as tunable tissue scaffolds, and microgel-based capsules for vascular drug delivery.

AUTHOR INFORMATION

Corresponding Author

*Phone: 404-894-4090. E-mail: lyon@gatech.edu.

Author Contributions

‖S.S. and C.E.H. are equally contributing authors.

Notes

The authors declare no competing financial interest.

Biographies

Shalini Saxena is a Ph.D. candidate in the School of Materials Science and Engineering at Georgia Tech. She received her B.S. in Chemical Engineering from Rose-Hulman in 2011.

Caroline E. Hansen is a Ph.D. candidate in the School of Chemistry and Biochemistry at Georgia Tech. She received her B.S. in Chemistry from Furman University in 2012.

L. Andrew Lyon is a Professor in the School of Chemistry and Biochemistry at Georgia Tech. He joined the GT faculty in 1999 after postdoctoral research at Penn State under the advisement of Michael Natan. He received his Ph.D. in Physical Chemistry from Northwestern University under the direction of Joseph Hupp and his B.A. in Chemistry from Rutgers College. He has been honored as a Beckman Young Investigator, Sloan Fellow, Dreyfus Teacher-Scholar, NSF CAREER recipient, and Fresenius Awardee.

ACKNOWLEDGMENTS

Funding for S.S. was provided by the NSF Integrative Graduate Education and Research Traineeship program in Stem Cell Biomanufacturing (0965945) and the NIH (R01GM088291). Additional funding from Georgia Tech and the GT/Emory/CHOA Center for Pediatric Nanomedicine is gratefully acknowledged.

REFERENCES

(1) Deshayes, S.; Kasko, A. M. Polymeric biomaterials with engineered degradation. *J. Polym. Sci., Part A: Polym. Chem.* **2013**, *51*, 3531–3566.

(2) Galperin, A.; Long, T. J.; Ratner, B. D. Degradable, Thermo-Sensitive Poly(*N*-isopropyl acrylamide)-Based Scaffolds with Controlled Porosity for Tissue Engineering Applications. *Biomacromolecules* **2010**, *11*, 2583–2592.

(3) Bryers, J. D.; Giachelli, C. M.; Ratner, B. D. Engineering biomaterials to integrate and heal: The biocompatibility paradigm shifts. *Biotechnol. Bioeng.* **2012**, *109*, 1898–1911.

(4) Saunders, B. R.; Laajam, N.; Daly, E.; Teow, S.; Hu, X.; Stepto, R. Microgels: From responsive polymer colloids to biomaterials. *Adv. Colloid Interface Sci.* **2009**, *147–148*, 251–262.

(5) Wang, Y.-X.; Robertson, J.; Spillman, W., Jr.; Claus, R. Effects of the Chemical Structure and the Surface Properties of Polymeric Biomaterials on Their Biocompatibility. *Pharm. Res.* **2004**, *21*, 1362–1373.

(6) Champion, J.; Walker, A.; Mitragotri, S. Role of Particle Size in Phagocytosis of Polymeric Microspheres. *Pharm. Res.* **2008**, *25*, 1815−1821.
(7) Champion, J. A.; Katare, Y. K.; Mitragotri, S. Particle shape: A new design parameter for micro- and nanoscale drug delivery carriers. *J. Controlled Release* **2007**, *121*, 3−9.
(8) Drummond, D. C.; Meyer, O.; Hong, K.; Kirpotin, D. B.; Papahadjopoulos, D. Optimizing Liposomes for Delivery of Chemotherapeutic Agents to Solid Tumors. *Pharmacol. Rev.* **1999**, *51*, 691−744.
(9) Mitragotri, S.; Lahann, J. Physical approaches to biomaterial design. *Nat. Mater.* **2009**, *8*, 15−23.
(10) Rehfeldt, F.; Engler, A. J.; Eckhardt, A.; Ahmed, F.; Discher, D. E. Cell responses to the mechanochemical microenvironment—Implications for regenerative medicine and drug delivery. *Adv. Drug Delivery Rev.* **2007**, *59*, 1329−1339.
(11) Discher, D. E.; Janmey, P.; Wang, Y. L. Tissue cells feel and respond to the stiffness of their substrate. *Science* **2005**, *310*, 1139−1143.
(12) Bae, K. H.; Wang, L.-S.; Kurisawa, M. Injectable biodegradable hydrogels: progress and challenges. *J. Mater. Chem. B* **2013**, *1*, 5371−5388.
(13) Tibbitt, M. W.; Anseth, K. S. Hydrogels as extracellular matrix mimics for 3D cell culture. *Biotechnol. Bioeng.* **2009**, *103*, 655−663.
(14) Kharkar, P. M.; Kiick, K. L.; Kloxin, A. M. Designing degradable hydrogels for orthogonal control of cell microenvironments. *Chem. Soc. Rev.* **2013**, *42*, 7335−7372.
(15) Merkel, T. J.; Jones, S. W.; Herlihy, K. P.; Kersey, F. R.; Shields, A. R.; Napier, M.; Luft, J. C.; Wu, H.; Zamboni, W. C.; Wang, A. Z.; Bear, J. E.; DeSimone, J. M. Using mechanobiological mimicry of red blood cells to extend circulation times of hydrogel microparticles. *Proc. Natl. Acad. Sci. U.S.A.* **2011**, *108*, 586−591.
(16) Jia, X.; Yeo, Y.; Clifton, R. J.; Jiao, T.; Kohane, D. S.; Kobler, J. B.; Zeitels, S. M.; Langer, R. Hyaluronic Acid-Based Microgels and Microgel Networks for Vocal Fold Regeneration. *Biomacromolecules* **2006**, *7*, 3336−3344.
(17) Dai, Z.; Ngai, T. Microgel particles: The structure-property relationships and their biomedical applications. *J. Polym. Sci., Part A: Polym. Chem.* **2013**, *51*, 2995−3003.
(18) Saunders, J. M.; Tong, T.; Le Maitre, C. L.; Freemont, T. J.; Saunders, B. R. A study of pH-responsive microgel dispersions: from fluid-to-gel transitions to mechanical property restoration for load-bearing tissue. *Soft Matter* **2007**, *3*, 486−494.
(19) Milani, A. H.; Freemont, A. J.; Hoyland, J. A.; Adlam, D. J.; Saunders, B. R. Injectable Doubly Cross-Linked Microgels for Improving the Mechanical Properties of Degenerated Intervertebral Discs. *Biomacromolecules* **2012**, *13*, 2793−2801.
(20) Hendrickson, G. R.; Smith, M. H.; South, A. B.; Lyon, L. A. Design of Multiresponsive Hydrogel Particles and Assemblies. *Adv. Funct. Mater.* **2010**, *20*, 1697−1712.
(21) Saunders, B. R. On the Structure of Poly(*N*-isopropylacrylamide) Microgel Particles. *Langmuir* **2004**, *20*, 3925−3932.
(22) Smith, M. H.; Herman, E. S.; Lyon, L. A. Network Deconstruction Reveals Network Structure in Responsive Microgels. *J. Phys. Chem. B* **2011**, *115*, 3761−3764.
(23) Gao, J.; Frisken, B. J. Cross-Linker-Free *N*-Isopropylacrylamide Gel Nanospheres. *Langmuir* **2003**, *19*, 5212−5216.
(24) South, A. B.; Lyon, L. A. Direct Observation of Microgel Erosion via in-Liquid Atomic Force Microscopy. *Chem. Mater.* **2010**, *22*, 3300−3306.
(25) Smith, M. H.; Lyon, L. A. Tunable Encapsulation of Proteins within Charged Microgels. *Macromolecules* **2011**, *44*, 8154−8160.
(26) Jones, C. D.; Lyon, L. A. Synthesis and Characterization of Multiresponsive Core−Shell Microgels. *Macromolecules* **2000**, *33*, 8301−8306.
(27) Berndt, I.; Richtering, W. Doubly Temperature Sensitive Core−Shell Microgels. *Macromolecules* **2003**, *36*, 8780−8785.
(28) Jones, C. D.; Lyon, L. A. Shell-Restricted Swelling and Core Compression in Poly(*N*-isopropylacrylamide) Core−Shell Microgels. *Macromolecules* **2003**, *36*, 1988−1993.
(29) Berndt, I.; Popescu, C.; Wortmann, F.-J.; Richtering, W. Mechanics versus Thermodynamics: Swelling in Multiple-Temperature-Sensitive Core−Shell Microgels. *Angew. Chem., Int. Ed.* **2006**, *45*, 1081−1085.
(30) Gaulding, J.; South, A.; Lyon, L. A. Hydrolytically degradable shells on thermoresponsive microgels. *Colloid Polym. Sci.* **2013**, *291*, 99−107.
(31) Iyer, A. S. J.; Lyon, L. A. Self-Healing Colloidal Crystals. *Angew. Chem., Int. Ed.* **2009**, *48*, 4562−4566.
(32) Banquy, X.; Suarez, F.; Argaw, A.; Rabanel, J.-M.; Grutter, P.; Bouchard, J.-F.; Hildgen, P.; Giasson, S. Effect of mechanical properties of hydrogel nanoparticles on macrophage cell uptake. *Soft Matter* **2009**, *5*, 3984−3991.
(33) Deen, W. M.; Lazzara, M. J.; Myers, B. D. Structural determinants of glomerular permeability. *Am. J. Physiol.: Renal Physiol.* **2001**, *281*, F579−F596.
(34) Lau, C.; Sudbury, I.; Thomson, M.; Howard, P. L.; Magil, A. B.; Cupples, W. A. Salt-resistant blood pressure and salt-sensitive renal autoregulation in chronic streptozotocin diabetes. *Am. J. Physiol.: Regul., Integr. Comp. Physiol.* **2009**, *296*, R1761−1770.
(35) Hendrickson, G. R.; Lyon, L. A. Microgel Translocation through Pores under Confinement. *Angew. Chem., Int. Ed.* **2010**, *49*, 2193−2197.
(36) Holden, D. A.; Hendrickson, G. R.; Lan, W.-J.; Lyon, L. A.; White, H. S. Electrical signature of the deformation and dehydration of microgels during translocation through nanopores. *Soft Matter* **2011**, *7*, 8035−8040.
(37) Gaulding, J. C.; Spears, M. W.; Lyon, L. A. Plastic deformation, wrinkling, and recovery in microgel multilayers. *Polym. Chem.* **2013**, *4*, 4890−4896.
(38) Yamato, M.; Utsumi, M.; Kushida, A.; Konno, C.; Kikuchi, A.; Okano, T. Thermo-Responsive Culture Dishes Allow the Intact Harvest of Multilayered Keratinocyte Sheets without Dispase by Reducing Temperature. *Tissue Eng.* **2001**, *7*, 473−480.
(39) Schmidt, S.; Zeiser, M.; Hellweg, T.; Duschl, C.; Fery, A.; Möhwald, H. Adhesion and Mechanical Properties of PNIPAM Microgel Films and Their Potential Use as Switchable Cell Culture Substrates. *Adv. Funct. Mater.* **2010**, *20*, 3235−3243.
(40) Saxena, S.; Spears, M. W., Jr.; Yoshida, H.; Gaulding, J. C.; Garcia, A. J.; Lyon, L. A. Microgel film dynamics modulate cell adhesion behavior. *Soft Matter* **2014**, *10*, 1356−1364.